A method of inferring changes in deep ocean currents from satellite measurements of time-variable gravity

John M. Wahr

Department of Physics and Cooperative Institute for Research in Environmental Sciences,
University of Colorado, Boulder, Colorado, USA

Steven R. Jayne[1]

Department of Physics and Cooperative Institute for Research in Environmental Sciences,
University of Colorado, Boulder, Colorado, USA

Climate and Global Dynamics Division, National Center for Atmospheric Research, Boulder, Colorado, USA

Frank O. Bryan

Climate and Global Dynamics Division, National Center for Atmospheric Research, Boulder, Colorado, USA

[1]   The NASA/Deutsches Zentrum für Luft- und Raumfahrt (DLR) satellite gravity mission Gravity Recovery and Climate Experiment (GRACE), launched in March 2002, will map the Earth's gravity field at scales of a few hundred kilometers and greater every 30 days. We describe a method of using those gravity measurements to estimate temporal variations in deep ocean currents. We examine the probable accuracy of the current estimates by constructing synthetic GRACE data, based in part on output from an ocean general circulation model. We ignore the possible contamination caused by short-period gravity signals aliasing into the 30-day solutions. We conclude that in the absence of aliasing, GRACE should be able to recover the 30-day variability of midlatitude currents at a depth of 2 km with an error of about 6–15% in variance when smoothed with 500–700 km averaging radii.   *INDEX TERMS:* 1214 Geodesy and Gravity: Geopotential theory and determination; 4512 Oceanography: Physical: Currents; 4294 Oceanography: General: Instruments and techniques; 0305 Atmospheric Composition and Structure: Aerosols and particles (0345, 4801); 0370 Atmospheric Composition and Structure: Volcanic effects (8409); 0360 Atmospheric Composition and Structure: Transmission and scattering of radiation

1. Introduction

[2]   The Global Ocean Observing System (GOOS) will form the cornerstone of observational physical oceanography in the coming years. This system will be comprised of several components. Some will be measurements from remote sensing instruments, i.e., sea surface height from satellite altimetry (the Jason mission), while others will be in situ observations, as in the temperature and salinity profiles of the upper ocean from randomly drifting floats (the Argo program). The Argo float program and the Jason altimeter program are meant to complement each other. In addition to the vertical profiles of temperature and salinity, the Argo floats will provide direct observations of the ocean's velocity field at a depth of 2000 m. This will provide the first global map of subsurface velocities. In this paper we show that information about deep ocean currents can also be provided by the Gravity Recovery and Climate Experiment (GRACE) satellite gravity mission. We quantify the error characteristics of the GRACE velocity estimates as an initial step in learning how and to what degree the GRACE and Argo systems will complement one another and to what degree they will be redundant.

[3]   GRACE, jointly sponsored by NASA and the Deutsches Zentrum für Luft- und Raumfahrt (DLR), was launched in March 2002 and has a nominal lifetime of five years. The mission consists of two satellites, separated by about 220 km, in identical orbits with initial altitudes near 500 km. The satellites range to each other using microwaves, and the geocentric position of each spacecraft is monitored using onboard GPS receivers. Onboard accelerometers detect the nongravitational acceleration so that its effects can be removed from the satellite-to-satellite distance measurements. The residuals will be used to map the Earth's gravity field orders of magnitude more accurately, and to considerably higher spatial resolution, than by any previous satellite. GRACE will provide maps of the gravity field every 30 days. This will permit monthly variations in gravity to be determined down to scales of a few hundred

---

[1]Now at Physical Oceanography Department, Woods Hole Oceanographic Institution, Woods Hole, Massachusetts, USA.

kilometers and larger. These gravity variations can be used to study a variety of processes that involve redistribution of mass within the Earth or on its surface. Comprehensive descriptions of the expected performance of GRACE and various possible applications are given by *Dickey et al.* [1997] and *Wahr et al.* [1998].

[4] GRACE estimates of time-variable gravity over the ocean can be used to infer changes in ocean bottom pressure [*Dickey et al*, 1997; *Wahr et al.*, 1998; *Ponte*, 1999; *Johnson et al.*, 2001; *Wunsch et al.*, 2001]. The objective of this paper is to show how those estimates can be combined with the assumption of geostrophy to learn about the time variability of deep ocean currents. The temporal and spatial resolutions of the estimated currents will be the same as for the GRACE gravity field: 30-days and several hundred km. The coverage will be global, although the results will be less accurate near coasts (due to contamination from the hydrological mass signal over land) and near the equator (where the geostrophic assumption is not valid).

[5] First, we describe our proposed method of using the GRACE gravity estimates to infer deep ocean currents. We then assess the likely accuracy of the results, using synthetic GRACE data based in part on output from a general circulation model of the ocean.

2. A Method for Inferring Deep Ocean Currents From GRACE

[6] The linearized Navier–Stokes equation for the ocean, using the Boussinesq approximation, is of the form

$$\rho_0[\partial_t \mathbf{v} + 2\Omega \times \mathbf{v}] = -\nabla P + \mathcal{F} \qquad (1)$$

where ρ_0 is the mean oceanic density, $\mathbf{v}$ is the particle velocity, Ω is the Earth's angular velocity of rotation, P is the pressure, and $\mathcal{F}$ includes the external and frictional forcing terms. For periods $\gg 1$ day, and away from oceanic boundaries (the coasts, the seafloor, the sea surface) so that the effects of friction and external forcing are less important, (1) reduces to the geostrophic approximation:

$$2\rho_0 \Omega \times \mathbf{v} \approx -\nabla P \qquad (2)$$

[7] In the shallow water limit the vertical velocity is negligible compared with the horizontal velocities, and (2) reduces to

$$v_{south}(\theta, \phi, z) \approx -\frac{1}{2\Omega\rho_0 a \cos\theta \sin\theta} \partial_\phi P(\theta, \phi, z) \qquad (3)$$

$$v_{east}(\theta, \phi, z) \approx \frac{1}{2\Omega\rho_0 a \cos\theta} \partial_\theta P(\theta, \phi, z) \qquad (4)$$

where v_{south} and v_{east} are the southward and eastward currents, θ and ϕ are the colatitude and eastward longitude, z is the depth, and a is the mean radius of the Earth. If the pressure field at depth z is known, it can be used in (3) and (4) to estimate the currents at that depth. Note that (3) and (4) are not useful near the equator, where $\cos\theta \to 0$. There the Coriolis force is negligible and so the geostrophic assumption is not valid.

[8] As we will show, the GRACE gravity field measurements can be used to estimate changes in bottom pressure. This raises the possibility of using those estimates in (3) and (4) to deduce changes in currents at the seafloor. One complication is that the θ and ϕ derivatives of pressure in (3) and (4) are computed by holding the depth, z, constant. The bottom pressure, though, is defined on the surface $z = -H(\theta, \phi)$, where $H(\theta, \phi)$ is the depth of the ocean at (θ, ϕ). So, if we denote the fixed-depth derivatives in (3) and (4) by $\partial_\theta P|_{z=const}$ and $\partial_\phi P|_{z=const}$, and the bottom pressure by $P_{bott}(\theta, \phi)$, then by the chain rule:

$$\partial_\theta P|_{z=const} = \partial_\theta P_{bott} + (\partial_z P)(\partial_\theta H) = \partial_\theta P_{bott} - \rho_{bott} g \partial_\theta H \qquad (5)$$

with a similar equation for $\partial_\phi P|_{z=const}$, where ρ_{bott} is the density at the seafloor and g is the mean gravitational acceleration at the Earth's surface ($=9.82$ m/s^2). The last equality in (5) follows from the hydrostatic assumption

$$\partial_z P = -\rho g \qquad (6)$$

[9] To directly apply (3) and (4) to compute the geostrophic current at the bottom would require not just the bottom pressure, but also the bottom density. We avoid this complexity by computing the monthly changes in geostrophic currents on a constant depth surface (taken to be 2000 m) by constructing a proxy for the pressure changes at that depth based on the GRACE estimate of P_{bott}. As we show below, this works in practice because the monthly changes in the density field between the deep reference level and the bottom are small.

[10] Equations (3) and (4) can be used as follows to estimate changes in deep ocean currents from GRACE gravity data. It is usual to expand the geoid height, N, as a sum of associated normalized Legendre functions, $\tilde{P}_{lm}$, in the form [see, e.g., *Chao and Gross*, 1987]:

$$N(\theta, \phi) = a \sum_{l=0}^{\infty} \sum_{m=0}^{l} \tilde{P}_{lm}(\cos\theta)[C_{lm}\cos(m\phi) + S_{lm}\sin(m\phi)],$$

$$(7)$$

where the C_{lm}'s and S_{lm}'s are dimensionless Stokes' coefficients. GRACE measurements will be used to determine the C_{lm}'s and S_{lm}'s up to degree and order (i.e., l and m) = 100 every 30 days. For each $\tilde{P}_{lm}$ term in this expansion, the horizontal scale (half-wavelength) is approximately $20,000/l$ km.

[11] Observed changes in the C_{lm}'s and S_{lm}'s, denoted here as ΔC_{lm} and ΔS_{lm}, can be used to learn about variations in the Earth's mass distribution. For example, GRACE will detect changes in the Stokes' coefficients caused by changes in the distribution of mass within a thin layer at the Earth's surface (for example, in the ocean or atmosphere, or in the storage of water, snow, or ice on continents). Define the change in surface mass density, $\Delta\sigma$, as the vertical integral of the change in density, $\Delta\rho$, through this surficial layer:

$$\Delta\sigma(\theta, \phi) = \int_{\text{thin layer}} \Delta\rho(\theta, \phi, z) dz \qquad (8)$$

where z is the depth through the layer. For an oceanic region, the change in bottom pressure is $\Delta P_{bott}(\theta, \phi) = g\Delta\sigma(\theta, \phi)$. Using equation (14) of *Wahr et al.* [1998], we find:

$$\Delta P_{bott}(\theta, \phi) = \frac{ag\rho_E}{3} \sum_{l=0}^{\infty} \sum_{m=-l}^{l} \frac{(2l+1)}{(1+k_l)} \tilde{P}_{lm}(\cos\theta)[\Delta C_{lm}\cos(m\phi)$$

$$+ \Delta S_{lm}\sin(m\phi)], \quad (9)$$

where ρ_E is the mean density of the Earth (= 5517 kg/m^3), and the k_l are load Love numbers representing the response of the solid Earth to surface loads. Here, we use values of the k_l computed by D. Han (personal communication, 1998), and summarized by *Wahr et al.* [1998, Table 1].

[12] Substituting the expansion (9) into the geostrophic equations (3) and (4) (ignoring the difference between $\partial_\theta P|_{z=const}$ and $\partial_\theta P_{bott}$, and between $\partial_\phi P|_{z=const}$ and $\partial_\phi P_{bott}$ as discussed above), we obtain, after some algebra, a Legendre function expansion for changes in the horizontal components of bottom currents:

$$\Delta v_{south}(\theta, \phi) = \frac{1}{\cos\theta\sin\theta} \sum_{l,m} \tilde{P}_{lm}(\cos\theta)[\Delta C_{lm}^{south}\cos(m\phi)$$

$$+ \Delta S_{lm}^{south}\sin(m\phi)] \quad (10)$$

and

$$\Delta v_{east}(\theta, \phi) = \frac{1}{\cos\theta\sin\theta} \sum_{l,m} \tilde{P}_{lm}(\cos\theta)[\Delta C_{lm}^{east}\cos(m\phi)$$

$$+ \Delta S_{lm}^{east}\sin(m\phi)] \quad (11)$$

where

$$\begin{Bmatrix} \Delta C_{lm}^{south} \\ \Delta S_{lm}^{south} \end{Bmatrix} = \frac{g\rho_E}{6\Omega\rho} \frac{m(2l+1)}{1+k_l} \begin{Bmatrix} -\Delta S_{lm} \\ \Delta C_{lm} \end{Bmatrix} \quad (12)$$

and

$$\begin{Bmatrix} \Delta C_{lm}^{east} \\ \Delta S_{lm}^{east} \end{Bmatrix} = \frac{g\rho_E}{6\Omega\rho} \left[\frac{l-1}{1+k_{l-1}} \left[\frac{(l^2-m^2)(2l-1)}{2l+1} \right]^{1/2} \begin{Bmatrix} \Delta C_{l-1m} \\ \Delta S_{l-1m} \end{Bmatrix} \right.$$

$$\left. - \frac{l+2}{1+k_{l+1}} \left[\frac{((l+1)^2-m^2)(2l+3)}{2l+1} \right]^{1/2} \begin{Bmatrix} \Delta C_{l+1m} \\ \Delta S_{l+1m} \end{Bmatrix} \right]. \quad (13)$$

GRACE results for changes in the Stokes' coefficients, ΔC_{lm} and ΔS_{lm}, can be used in (12) and (13) to obtain the expansion coefficients that describe variations in the currents.

[13] The accuracy of the GRACE C_{lm} and S_{lm} solutions decreases quickly enough at large l, that the use of (10) and (11) as written leads to inaccurate results. Instead, the GRACE data will best be used to provide spatial averages of v_{south} and v_{east}. Here, we use the following averaging method, described by *Wahr et al.* [1998].

[14] Define a Gaussian spatial-averaging kernel as

$$W(\gamma) = \frac{b}{2\pi} \frac{\exp[-b(1-\cos\gamma)]}{1-e^{-2b}} \quad (14)$$

[*Jekeli*, 1981], where γ can be any angle between 0 and 2π, and

$$b = \frac{\ln(2)}{\left(1 - \cos\left(r_{\frac{1}{2}}/a\right)\right)}. \quad (15)$$

Here, $r_{\frac{1}{2}}$ is the half-width of the Gaussian averaging function: i.e., when $\gamma = r_{\frac{1}{2}}/a$, $W(\gamma)$ has decreased to half its value at $\gamma = 0$.

[15] We define

$$\overline{\Delta v_{south}}(\theta, \phi) = \frac{1}{\cos\theta\sin\theta} \int W(\gamma)\Delta v_{south}(\theta', \phi')\cos\theta'\sin\theta' \, dA' \quad (16)$$

and

$$\overline{\Delta v_{east}}(\theta, \phi) = \frac{1}{\cos\theta\sin\theta} \int W(\gamma)\Delta v_{east}(\theta', \phi')\cos\theta'\sin\theta' \, dA' \quad (17)$$

where now γ is the angle between the points (θ, ϕ) and (θ', ϕ') (i.e., $\cos\gamma = \cos\theta\cos\theta' + \sin\theta\sin\theta'\cos(\phi - \phi')$), and dA' is an element of solid angle ($dA' = \sin\theta' \, d\theta' \, d\phi'$). We refer to $\overline{\Delta v_{south}}$ and $\overline{\Delta v_{cast}}$ as spatial averages of Δv_{south} and Δv_{east}, although note that Δv_{south} and Δv_{east} have been multiplied by $\cos\theta'\sin\theta'$ before averaging. Using the expansions (10) and (11) in (16) and (17), we obtain

$$\overline{\Delta v_{south}}(\theta, \phi) = \frac{1}{\cos\theta\sin\theta} \sum_{l,m} 2\pi W_l \tilde{P}_{lm}(\cos\theta)[\Delta C_{lm}^{south}\cos(m\phi)$$

$$+ \Delta S_{lm}^{south}\sin(m\phi)] \quad (18)$$

and

$$\overline{\Delta v_{east}}(\theta, \phi) = \frac{1}{\cos\theta\sin\theta} \sum_{l,m} 2\pi W_l \tilde{P}_{lm}(\cos\theta)[\Delta C_{lm}^{east}\cos(m\phi)$$

$$+ \Delta S_{lm}^{east}\sin(m\phi)] \quad (19)$$

where

$$W_l = \int_0^\pi W(\alpha)P_l(\cos\alpha)\sin\alpha \, d\alpha \quad (20)$$

and $P_l = \tilde{P}_{lm=0}/\sqrt{2l+1}$ are the Legendre polynomials. Recursion relations useful for finding the W_l's are derived by *Jekeli* [1981] and summarized by *Wahr et al.* [1998, equation (34)]. A large value of $r_{\frac{1}{2}}$ in (15) causes the W_l's to decrease rapidly with increasing l, so that contamination from inaccurate GRACE results for C_{lm} and S_{lm} at large l is suppressed in (18) and (19).

[16] While we do use the GRACE Stokes' coefficients in (12), (13), (18), and (19), we interpret the results as estimates of changes in the currents at a fixed depth of 2000 meters, rather than at the seafloor. What, in effect, we are assuming is that changes in pressure at the seafloor—which is what the GRACE data provide—may be used as a proxy for changes in pressure at 2000 m depth, at least at periods of a few years or less. That is equivalent to assuming that most of the variability in the ocean's density distribution at these periods occurs above 2000 m. We choose that depth, somewhat arbitrarily, because it is the depth at which the Argo floats will drift [*Roemmich and Owens*, 2000].

[17] Recasting the problem as one of estimating the currents at a fixed depth rather than at the bottom avoids the complexity of the second term in the right-hand-side of (5). In addition, we expect the geostrophic estimate of the currents at that depth to be closer to the total currents than it would be at the seafloor. The geostrophic assumption is not likely to work well within about 100 meters of the seafloor, due to the presence of the frictional bottom boundary layer. Furthermore, the fact that the results must be averaged over scales of at least several hundred km to reduce the effects of GRACE measurement errors, reduces the usefulness of the bottom current results over much of the world's ocean, where the bathymetry varies at length scales that are of that order or smaller.

3. How Well Should This Method Work?

[18] The accuracy with which this method can be used to infer changes in currents at $\approx$2 km depth, depends on three factors: (1) whether changes in bottom pressure differ significantly or not from changes in pressure at 2 km depth; (2) whether changes in the currents at 2 km depth are nearly geostrophic; and (3) the characteristics of the errors in the GRACE bottom pressure estimates. We will look at the combined effects of all these errors in section 4. First, though, we look at each of these 3 factors separately.

3.1. Variation of Pressure With Depth

[19] Throughout this paper we use output from the POP (Parallel Ocean Program) ocean general circulation model described by *Dukowicz and Smith* [1994]. This is a free surface, primitive equation model, with an average horizontal grid spacing of 65 km and with 42 vertical levels. An anisotropic Smagorinsky eddy viscosity is used to represent horizontal dissipation [*Smagorinsky*, 1963; *Smith and McWilliams*, 2002], and bottom friction is parameterized with a quadratic bottom drag law with drag coefficient 10^{-3}. Vertical viscosity is calculated from the K-profile parameterization described by *Large et al.* [1994], and the effects of subgrid scale eddies are parameterized as in the work of *Gent and McWilliams* [1990]. The model is driven by an averaged annual cycle of monthly wind stress, surface heat flux, and surface salinity generated by the National Centers for Environmental Predication (NCEP) as described by *Large et al.* [1997]. Only one year of forcing fields are used, but they are cycled repeatedly through a multiyear modeling span.

[20] In this study we use model output from just one year (year 28) of the model period. The one-year mean is

removed from each field, so that we are only considering time-variable components. All fields are then averaged over successive 30 day periods, and it is those 30-day averages that are used in the analyses described in this paper. The rationale is that the gravity coefficients provided by GRACE will, similarly, be averages over 30 days.

[21] Figure 1a shows the root-mean square (RMS) of the 30-day averaged POP pressure fields at a depth of 2125 meters (the closest model level to 2000 m). There are three regions with significant variability, all at high latitudes: one in the northwestern Pacific and two in the Southern Ocean. These regions have been noted by others [*Stammer et al.*, 2000; *Tierney et al.*, 2000]. Figure 1b shows the RMS of the difference between the pressure at 2125 m and the bottom pressure. This difference, which is caused by changes in density between 2125 m and the seafloor, is much smaller than the pressure field itself. The region with large variability in the northwestern Pacific is not evident in Figure 1b. In fact, the large signals in all three of the high variability regions evident in Figure 1a appear to be caused mostly by variations in sea surface height, and so are largely barotropic in origin [*Stammer et al.*, 2000; *Tierney et al.*, 2000].

[22] Figure 2 shows the global RMS of the pressure field at each depth and the global RMS of the difference between the pressure at that depth and the pressure at the seafloor. The results show that the pressure variability at 2125 m depth and at the seafloor agree to within about 20% in global RMS, and so to within about $0.20^2 = 4\%$ in variance. This, then, is the level of error we might expect to be caused by using bottom pressure to calculate the geostrophic currents at 2125 m, rather than using the 2125 m pressure fields themselves. As we will see in the following section, however, this analysis underestimates the true error in the inferred currents caused by using this incorrect pressure field.

3.2. Are Deep Ocean Currents Geostrophic?

[23] We use the 30-day averages of the POP pressure fields in (3) and (4) to compute monthly changes in the geostrophic currents as a function of depth, and compare with changes in the 30-day averages of the POP current fields to determine whether monthly variations in those currents are close to geostrophic. We refer to the difference between the currents and the geostrophic approximation of the currents as the nongeostrophic currents. Figure 3a shows the RMS of the current amplitudes at 2125 m depth (the amplitude of the current vector is $\sqrt{\Delta v_{south}^2 + \Delta_{east}^2}$). Figure 3b shows the RMS of the nongeostrophic current amplitudes at that same depth. Latitudes within 10° of the equator are omitted in Figure 3 and in subsequent figures, to avoid saturating the contours near the equator where the geostrophic approximation becomes less accurate (see the discussion below (4)). The RMS values in Figure 3b are significantly smaller than the RMS values in Figure 3a, implying that geostrophy captures most of the variability in the currents at 2125 m depth.

[24] These results are summarized further in Figures 4a and 5a. Figure 4a shows values of the RMS integrated over 5° latitude bands, of the amplitude of the total currents (solid line) and of the nongeostrophic currents (dashed–
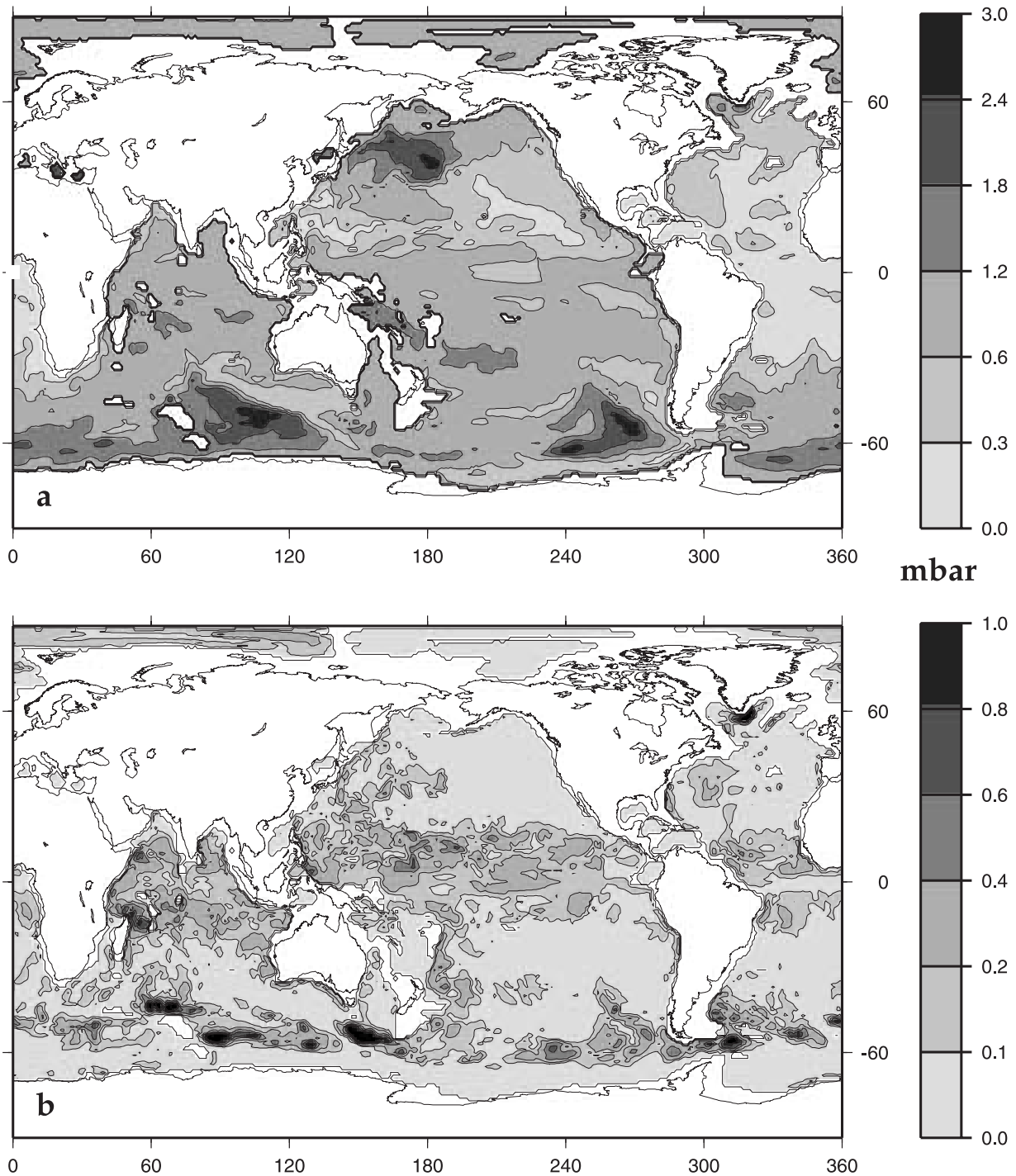
Figure 1. A map of the RMS, about the mean, of 30-day averages of one year of pressure fields from the POP model. (a) The RMS of the pressure at 2125 m depth. (b) The RMS of the difference between bottom pressure and the pressure at 2125 m depth.

dotted line). The nongeostrophic RMS values are so small they are barely evident on this plot, except between about 60°N and 65°N, where the ocean is quite narrow and the currents consist only of a few viscous boundary currents. Figure 5a shows the RMS values for the total and non-geostrophic currents integrated over the globe, but now as a function of depth (latitudes below 10° are not included). At a depth of 2125 m, the nongeostrophic currents are only

about 3% of the actual currents in global RMS, and so about $0.03^2 = 0.1\%$ in global variance. Note from Figure 5a that the geostrophic assumption appears to work well at depths below about 50 m, but that above 50 m the nongeostrophic currents are a significant fraction of the total currents. In this regime the wind stress is the primary contributor to the currents.

[25] Since the results here show that the geostrophic assumption works well at 2125 m depth, and the results
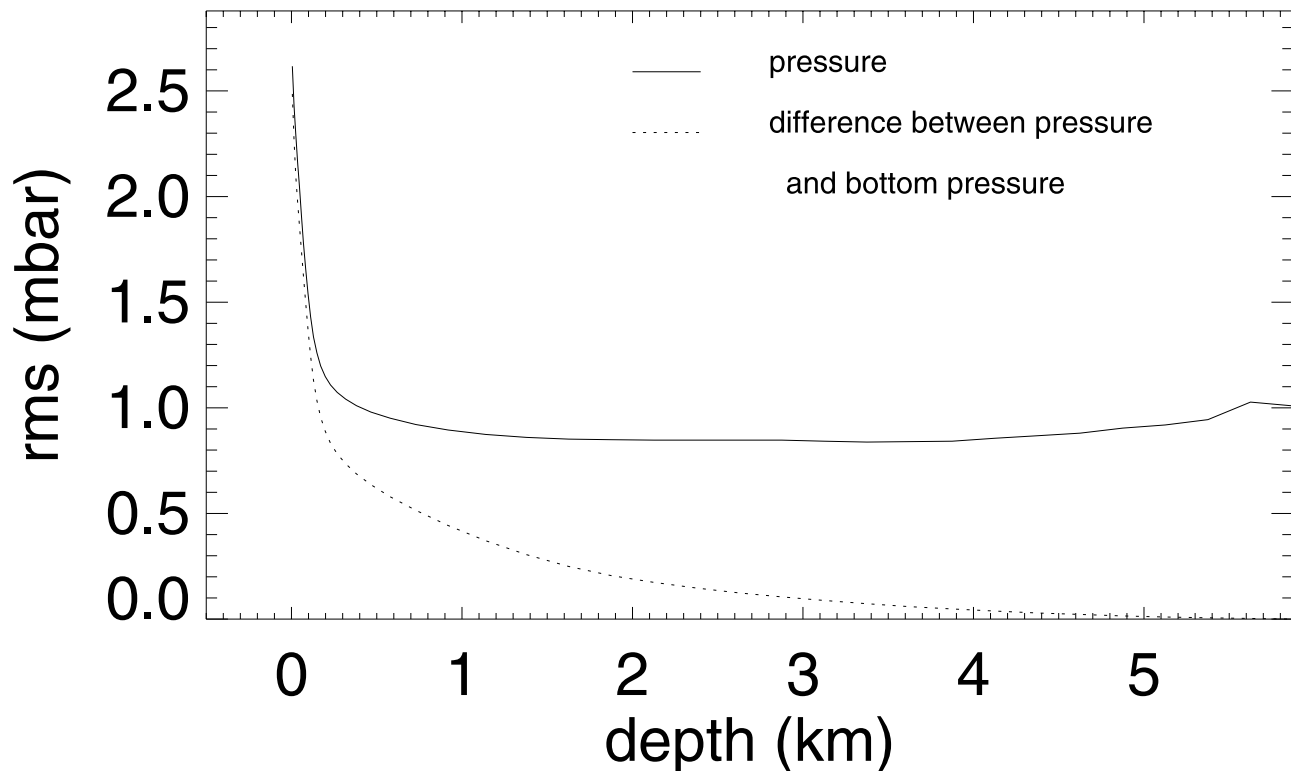
Figure 2. The global RMS of the time variability in the POP pressure fields, as a function of depth in the ocean. Shown, at every depth, is the RMS of pressure at that depth, and the RMS of the difference between pressure at that depth and bottom pressure.

in section 3.1 indicate that variations in bottom pressure and in the 2125 m pressure agree to within about 20% RMS, we might expect we could obtain estimates of changes in the 2125 m currents accurate to about 20% RMS by using bottom pressure variations in the geostrophic equations ((3) and (4)). This, though, is not the case over a large portion of the ocean.

[26] This can be seen by comparing the RMS of the total currents (Figure 3a) with Figure 3c, which shows the RMS of the difference between the 2125 m currents and the currents computed using bottom pressure variations in the geostrophic equations ((3) and (4)). We will refer to this latter approximation of the currents as the bottom geostrophic approximation. Although there are regions of the globe where the difference shown in Figure 3c is significantly smaller than the total signal, there are also regions where it is not.

[27] This is even more evident from Figures 4a and 5a, by comparing the RMS of the total current (solid lines) with the RMS difference between the total current and the bottom geostrophic approximation (dashed lines). Figure 5a, for example, shows that at a depth of 2125 m, the error obtained using the bottom geostrophic approximation is 80–85% of the total signal in global RMS.

[28] The reason the bottom geostrophic approximation does not work as well as anticipated from section 3.1, is related to the fact that deep ocean currents have considerably more power at short wavelengths than does the deep ocean pressure [see, e.g., *Chave, et al.*, 1992]. This is evident in Figure 6, which shows the degree variances of

monthly changes in pressure and in both components of the currents at 2125 m depth. If a function $f(\theta, \phi)$ is expanded as

$$f = \sum_{l=0}^{\infty} \sum_{m=0}^{l} \tilde{P}_{lm}(\cos \theta) [f_{clm} \cos(m\phi) + f_{slm} \sin(m\phi)], \quad (21)$$

the degree variance at any angular degree l is defined as

$$B_l = \sum_{m=0}^{l} \left(f_{clm}^2 + f_{slm}^2 \right). \quad (22)$$

B_l is the contribution to the global variance of f from all terms in (21) with angular degree l. Since the scale of any (l, m) term in (21) is roughly $20,000/l$ km, B_l represents the total contribution to the variance of f from all terms having that scale.

[29] Figure 6 shows that the power in the currents extends to much shorter wavelengths than does the power in the pressure fields. This can be understood by noting from the geostrophic approximation (3) and (4) (which, as we have shown, provides accurate estimates of the currents) that the currents are proportional to spatial derivatives of the pressure, and that differentiation amplifies short wavelengths relative to longer wavelengths.

[30] We conclude that the comparatively good agreement between bottom pressure and 2125 m pressure, as described in section 3.1, should be interpreted only as implying good agreement at the relatively long wavelengths that dominate the pressure field. We infer from the poor performance of
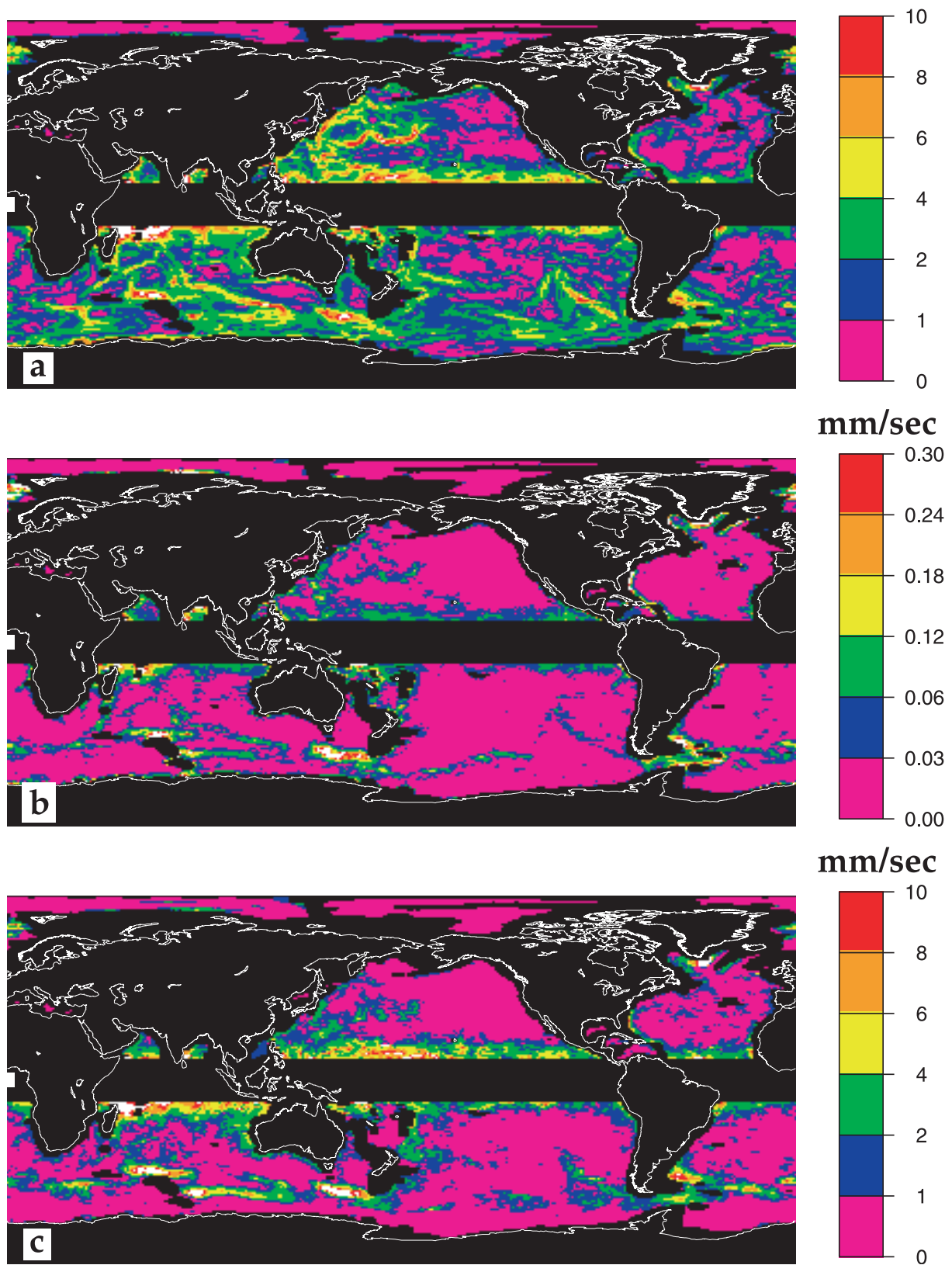
Figure 3. A map of the RMS, about the mean, of 30-day averages of one year of POP current amplitudes. (a) for the currents at 2125 m depth; (b) for the nongeostrophic currents at 2125 m depth; (c) for the difference between the 2125 m currents and the bottom geostrophic approximation.
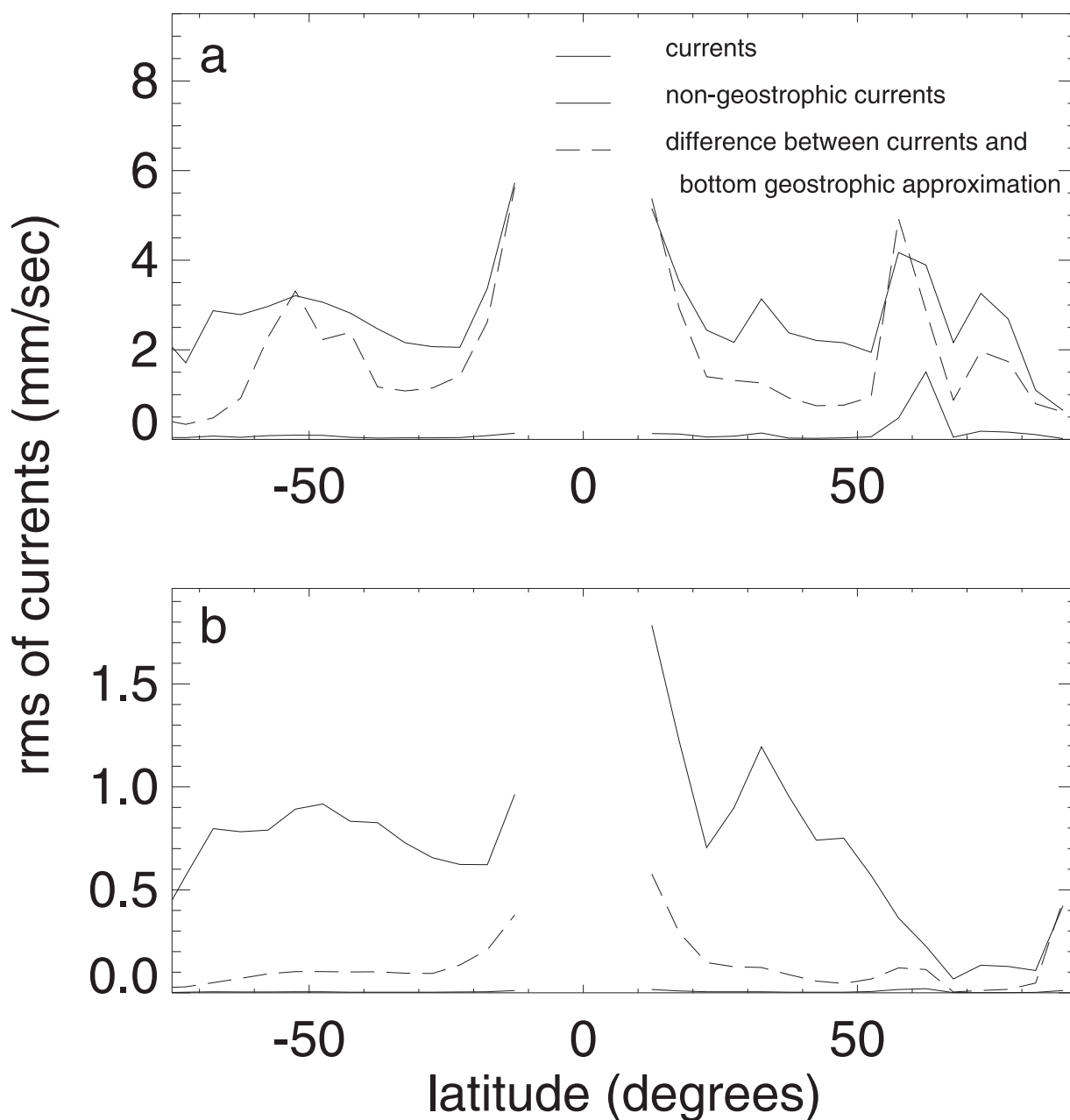
Figure 4. The global RMS of 30-day variability of one year of POP currents integrated over 5° latitude bands. Shown are the RMS of the currents at 2125 m; the RMS of the nongeostrophic currents at 2125 m; and the RMS of the difference between the 2125 m currents and the bottom geostrophic approximation. Results are shown for the unsmoothed POP output (a), and for smoothed fields computed using a 500-km Gaussian average (b).

the bottom geostrophic approximation, that the agreement between bottom pressure and 2125 m pressure must be worse at the shorter wavelengths that contribute most strongly to the deep currents.

[31] The poor agreement at short wavelengths is somewhat of a moot point for GRACE, however, since the mission will not provide accurate short wavelength gravity coefficients in any case. Instead, the GRACE data should only be used to estimate velocities averaged over scales of several hundred km and greater. The smoothing process (see (16) and (17)) removes much of the signal. For

example, when a Gaussian function with an averaging radius (r_1) of 500 km is used to smooth the 2125 m velocity fields, the global RMS of the smoothed fields is only about 30% of the global RMS of the unsmoothed fields, and so about 10% in variance. These RMS and variance ratios decrease further to 24% and 6% for an averaging radius of 700 km. At these relatively long scales, the variability in currents is primarily associated with seasonal changes in the general circulation of the ocean, the mesoscale variability essentially being completely filtered out by the spatial averaging.
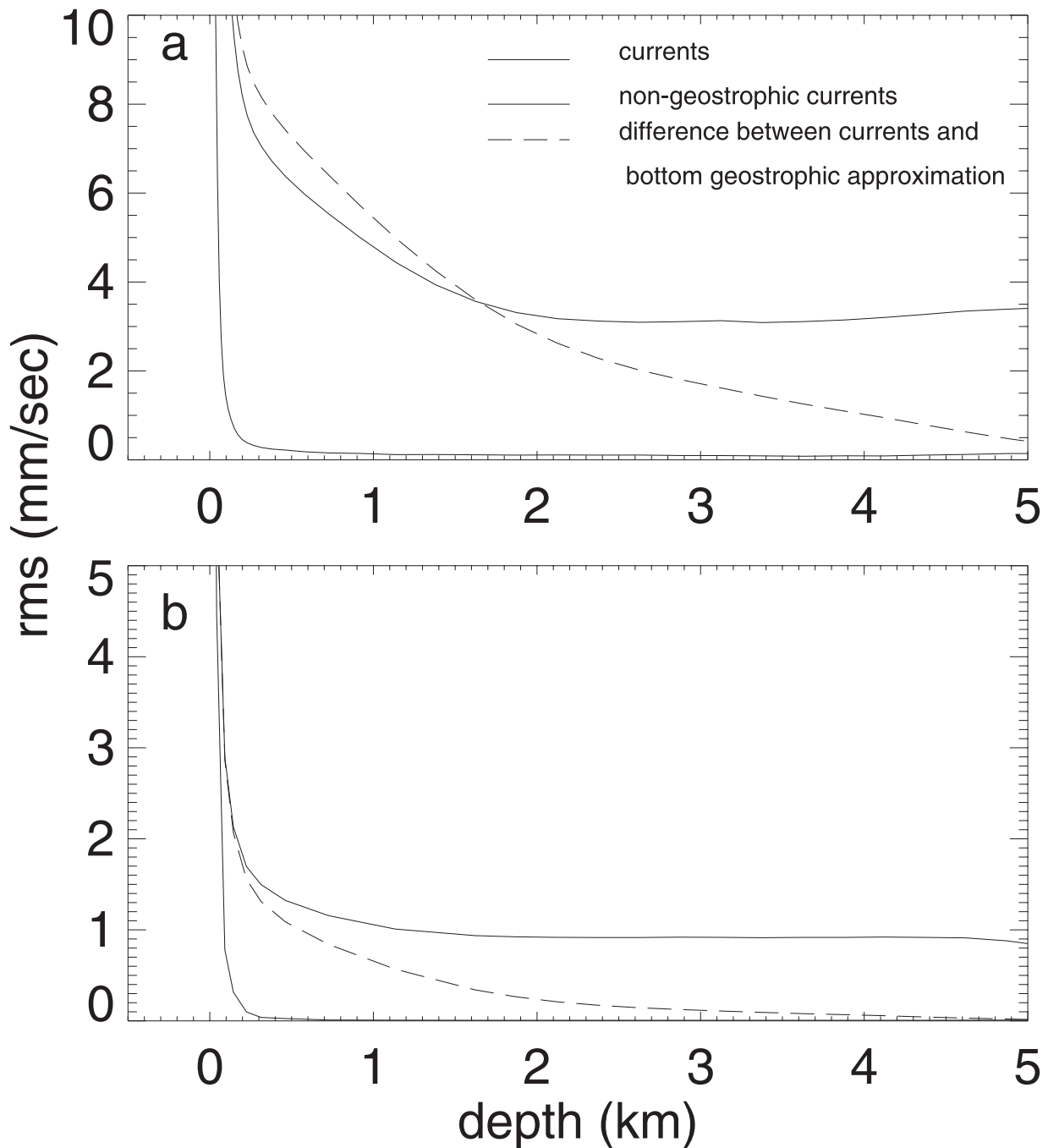
Figure 5. The global RMS of the time variability in the POP current fields, as a function of depth in the ocean. Shown, at every depth, is the RMS of the current amplitudes, the RMS of the amplitudes of the nongeostrophic currents, and the RMS of the amplitudes of the difference between the currents and the bottom geostrophic approximation. (a) The RMS values computed using the unsmoothed POP output. (b) The RMS values computed after smoothing the POP fields (both the actual currents and the geostrophic currents) using a Gaussian averaging function with a 500 km radius.

[32] On the other hand, the bottom geostrophic approximation does a better job of reproducing the long wavelengths present in the smoothed field, than it does the short wavelengths that dominate the unsmoothed field. This is evident in Figure 7, which shows RMS values for the 2125 m currents (a), the nongeostrophic currents (b), and the difference between the currents and the bottom geostrophic approximation of the currents (c); where in all cases the currents and their approximations have first been smoothed using a Gaussian averaging radius of 500 km. The errors in the bottom geostrophic approximation are now a noticeably smaller fraction of the total signal than in the unsmoothed case (Figure 3). Figures 4b and 5b further illustrate this improvement by showing the RMS results integrated over 5 latitude bands and over the entire globe, respectively. Note from Figure 5b that at 2125 m depth the global RMS error
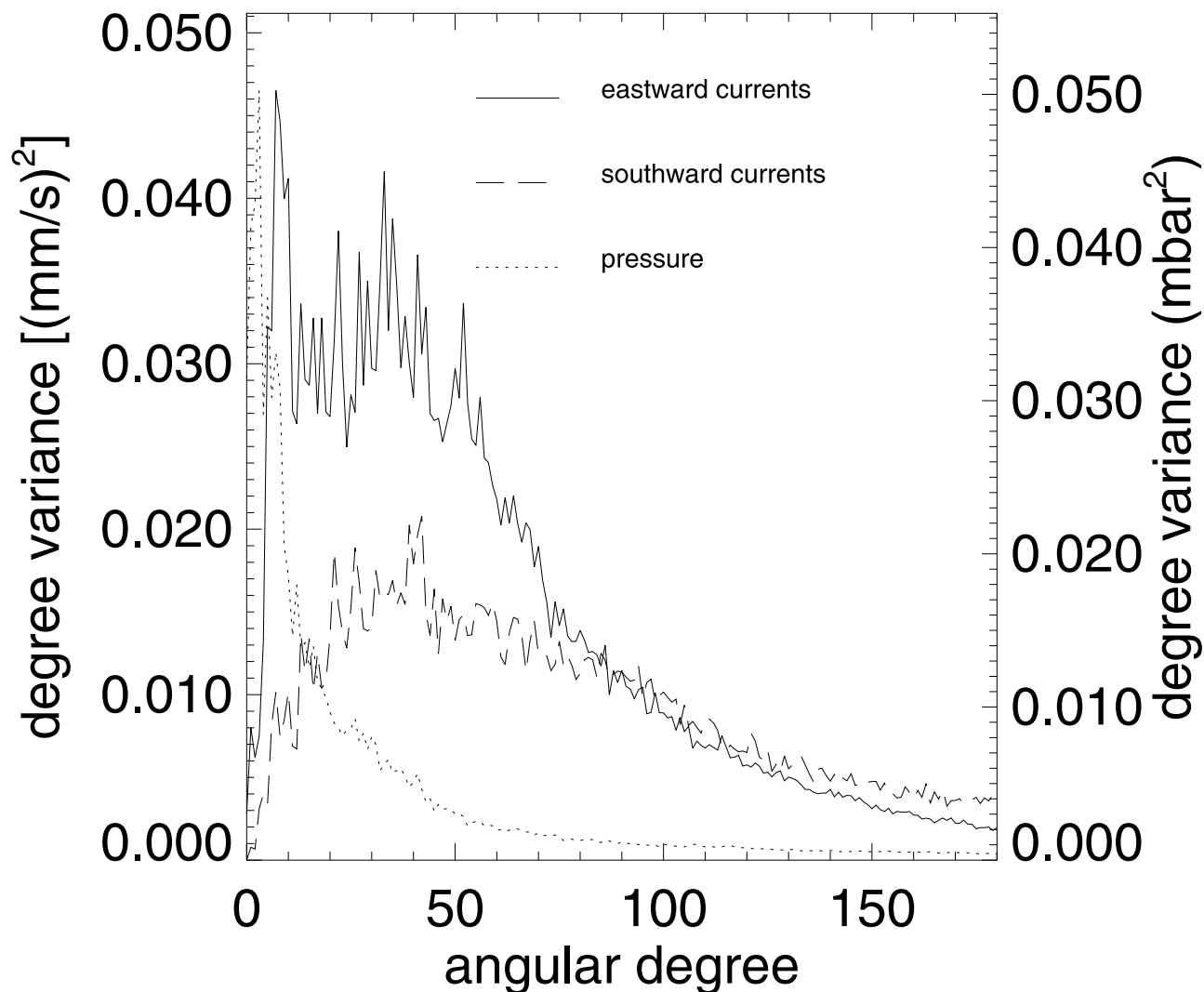
Figure 6. Degree variances of the 30-day variability of one year of POP fields. Shown are results for pressure and for the southward and eastward components of the currents, all at 2125 m depth. Each angular degree, l, corresponds to a horizontal scale of 20,000/l km Gaussian averaging function.

in the smoothed bottom geostrophic approximation is about 20% of the total smoothed currents. This is about the same relative difference as that between the bottom pressure and 2125 m pressure discussed in section 3.1.

[33] Figure 5b illustrates the improvement in the bottom geostrophic approximation at still deeper levels in the ocean. This improvement is simply due to the fact that at deeper levels, the pressure variability agrees more closely with the pressure variability at the seafloor. At a depth of 3 km, for example, the error in the bottom geostrophic approximation has been reduced to 12–14% of the total signal in global RMS. And at a depth of 4 km this relative error is only about 6–7%. As we will see in section 4, this level of improvement does not map directly into the improvement obtainable using GRACE data, because of errors in the GRACE estimates of bottom pressure.

3.3. GRACE Recovery of Bottom Pressure

[34] Our method of inferring changes in deep ocean currents, formulated in section 2, assumes that all varia-

tions in the GRACE Stokes' coefficients are caused by changes in the oceanic mass distribution. Equation (9), for example, is not strictly valid if there are observational errors in the GRACE C_{lm}, S_{lm} estimates, as there certainly will be. The averaging coefficients, W_l, are introduced into (18) and (19) to minimize the effects of these errors. Furthermore, contributions to the Stokes' coefficients caused by mass variability outside the oceans can contaminate the oceanic estimates. This latter problem is actually made more severe by the averaging process, especially at points where the averaging function extends well outside the ocean's boundaries.

[35] There are three sources of nonoceanic time-variable gravity that could contaminate the GRACE bottom pressure estimates: the solid Earth, the atmosphere, and the water, snow, and ice stored on land. For the solid Earth there are two signals large enough to have a significant effect. One is the elastic deformation caused by the ocean load itself. The effects of that deformation have already been included in the formalism developed in section 2, through the Love number k in (9), and later in (12) and (13).
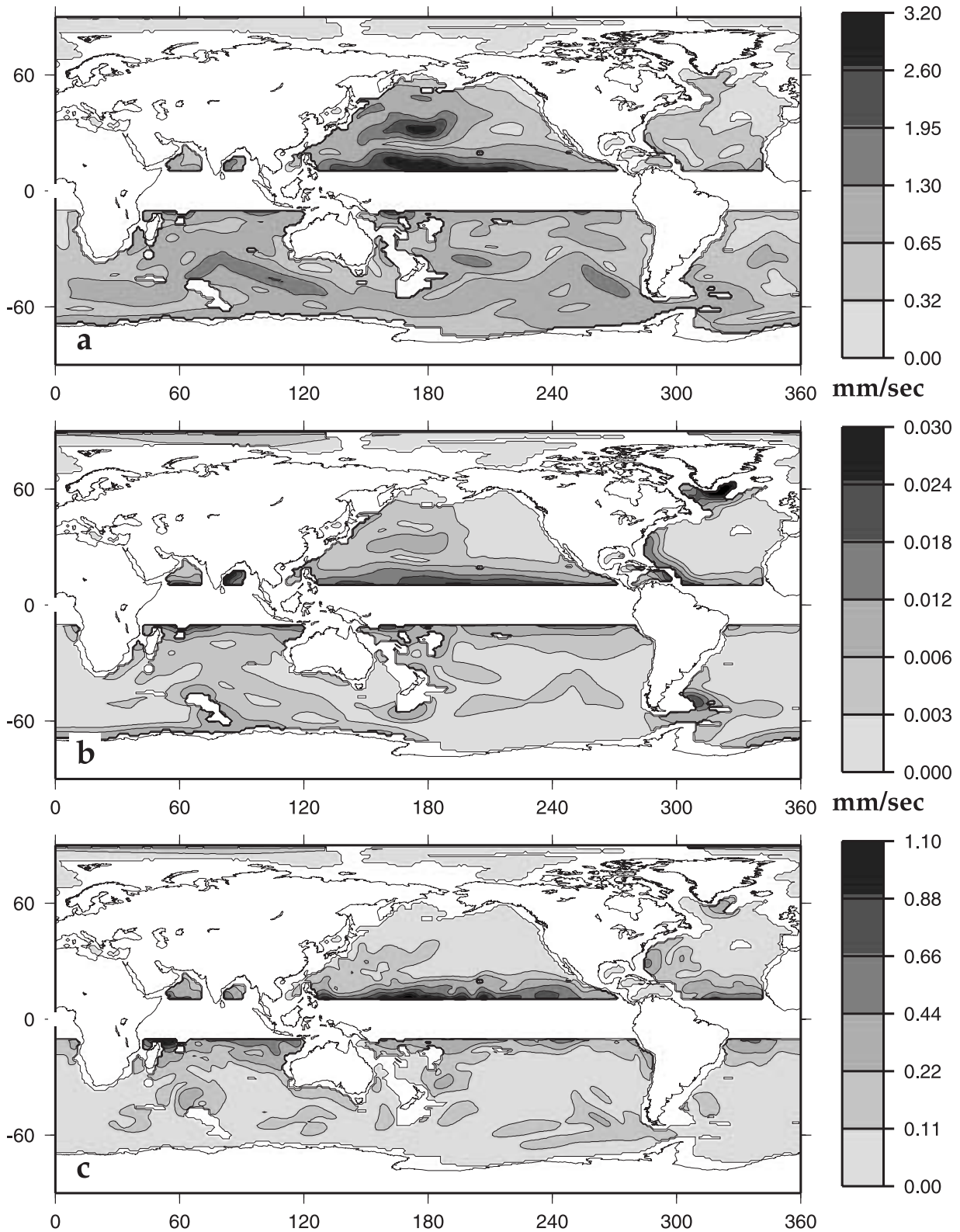
Figure 7. Similar to Figure 3, but after smoothing the POP currents (both the actual currents and the geostrophic currents) using a 500 km Gaussian averaging function.

[36] The other important solid Earth effect is post-glacial-rebound (PGR): the ongoing, viscoelastic response of the solid Earth to the deglaciation that occurred at the end of the last ice age. The PGR signal cannot be predicted well enough to allow it to be confidently removed from the data. It will appear as a secular bottom pressure signal in portions of the North Atlantic and North Pacific and in the southern ocean close to Antarctica, causing apparent amplitudes of

up to 0.3–0.5 mbar/yr in the high latitude deep ocean. Although this signal will contaminate attempts to infer secular changes in bottom pressure in these regions, it will have no effect on any nonsecular variability inferred from the GRACE data.

[37] The gravity signal caused by variability in the atmospheric density distribution is indistinguishable from that caused by a change in the density distribution in the underlying ocean or on land. Fortunately, the atmospheric signal can be independently estimated using global atmospheric pressure fields (or, for a somewhat better approximation, geopotential height fields: see *Swenson and Wahr* [2002]) generated by forecast centers such as the European Center for Medium Range Weather Forecasts (ECMWF). The GRACE project will use these fields to remove the atmospheric effects before releasing the data to users. But only the atmospheric contributions over land will be removed, not those over the ocean. The reason is that oceanic bottom pressure at any point is proportional to the total mass, oceanic plus atmospheric, integrated vertically above that point. So the gravitational contributions from the atmosphere above the ocean must be retained in the data to infer the bottom pressure.

[38] Still, there will be errors in the bottom pressure estimates due to errors in the atmospheric pressure fields over land. These errors will leak into the bottom pressure estimates, particularly near coasts, wherever the spatial averaging function used to reduce the effects of satellite errors extends over land.

[39] This atmospheric leakage is far less of a problem than the similar leakage caused by changes in the distribution of water, snow, and ice stored on land: the third, and largest, source of contamination. The hydrological mass signal causes a time-variable gravity signal over land that is typically several times the time-variable gravity signal over the ocean caused by changes in ocean mass [*Wahr et al.*, 1998].

[40] The contamination from the hydrology signal (and, concurrently, from the effects of atmospheric pressure errors over land) can be reduced by applying a technique described by *Wahr et al.* [1998, equations (35)–(39)]. Briefly, the GRACE gravity data are first used to solve for the mass distribution over continental regions, using a Gaussian averaging function. We find that a relatively short Gaussian radius, typically 100 km, appears to optimize the competing requirements of reducing the leakage from surrounding regions into the water storage estimates, while minimizing the impact of the satellite measurement errors on those estimates. The gravity signal caused by this inferred continental mass distribution is then removed from the GRACE results, and the residuals are used to solve for bottom pressure.

[41] Figure 8 shows the effectiveness of this procedure. We construct one year of synthetic, 30-day GRACE Stokes' coefficients by including contributions from ocean bottom pressure using the output from the POP model described above; of continental water storage over all regions except Antarctica using the global, gridded results of A. B. Shmakin et al. (Global modeling of land water and energy balances, 3, Interannual variability, submitted to *Journal of Hydrometeorology*, 2002); of changes in snow mass over Antarctica using monthly, gridded, accumulation fields generated by the CSM-1 climate model developed at the

National Center for Atmospheric Research [see, e.g., *Briegleb and Bromwich*, 1998]; of errors in atmospheric pressure over land, obtained by taking differences between the gridded pressure fields produced by the ECMWF and those produced by the National Meteorological Center (NMC), divided by $\sqrt{2}$ (see *Wahr et al.* [1998] for a discussion of this method of approximating atmospheric pressure errors); and of GRACE measurement errors, using error estimates provided by B. Thomas and M. Watkins (personal communication, 1998) [see also *Wahr et al.*, 1998], that are consistent with those described in the GRACE Science and Mission Requirements Document [*Jet Propulsion Laboratory*, 2001]. The estimates of the GRACE measurement errors do not include the possible effects of temporal aliasing of short-period geophysical signals into the 30-day averages. This issue is briefly discussed in section 5.

[42] We use these simulated Stokes' coefficients to estimate Gaussian averages of monthly changes in bottom pressure, and compare the results with the correct Gaussian-averaged bottom pressure variations, obtained using the bottom pressure fields that went into the simulation. Figure 8a shows a global map of the correct bottom pressure, smoothed using a Gaussian radius of 500 km. Figure 8b shows the RMS of the difference between the estimates retrieved from GRACE and the correct results. These RMS values, which can be interpreted as the errors in the GRACE recovery of monthly changes in bottom pressure, are substantially smaller than the RMS of the expected signal except within about 500 km of the coast. Within that region, the RMS of the errors shown in Figure 8b is about 2 mbar, as large as the largest RMS values of the signal shown in Figure 8a.

[43] Figure 8c shows a global map of the RMS difference between the GRACE bottom pressure estimates and the correct bottom pressure, but now after first correcting for the continental signal as described above. The contamination is still evident along the coasts, but has been substantially reduced. The RMS of the errors within 500 km of the coast is now only 0.4 mbar.

[44] The estimate, in mbars, of the error caused by the continental contamination is dependent almost entirely on the hydrology model used in the simulation. There are large uncertainties in any water storage model, and so these error estimates are approximate, at best. But our conclusion that we are able to reduce the RMS of the contamination near coasts to about (0.4 mbar)/(2.0 mbar) = 20% of its original value, is probably independent of the water storage model.

4. A Full Simulation

[45] We use the synthetic GRACE Stokes' coefficients described in section 3.3, in (12)(13), (18), and (19), to estimate changes in 30-day averages of the 2125 m currents. We choose a 500 km radius for the Gaussian averaging kernel. We compare the results with the corresponding Gaussian averages of the correct 2125 m currents, obtained by using, in (16) and (17), the 2125 m currents predicted by the same POP run that generated the bottom pressure fields used in the GRACE simulation. The difference between the results is an estimate of the total error in the GRACE recovery of monthly changes in 2125 m currents, combining all the error sources described in
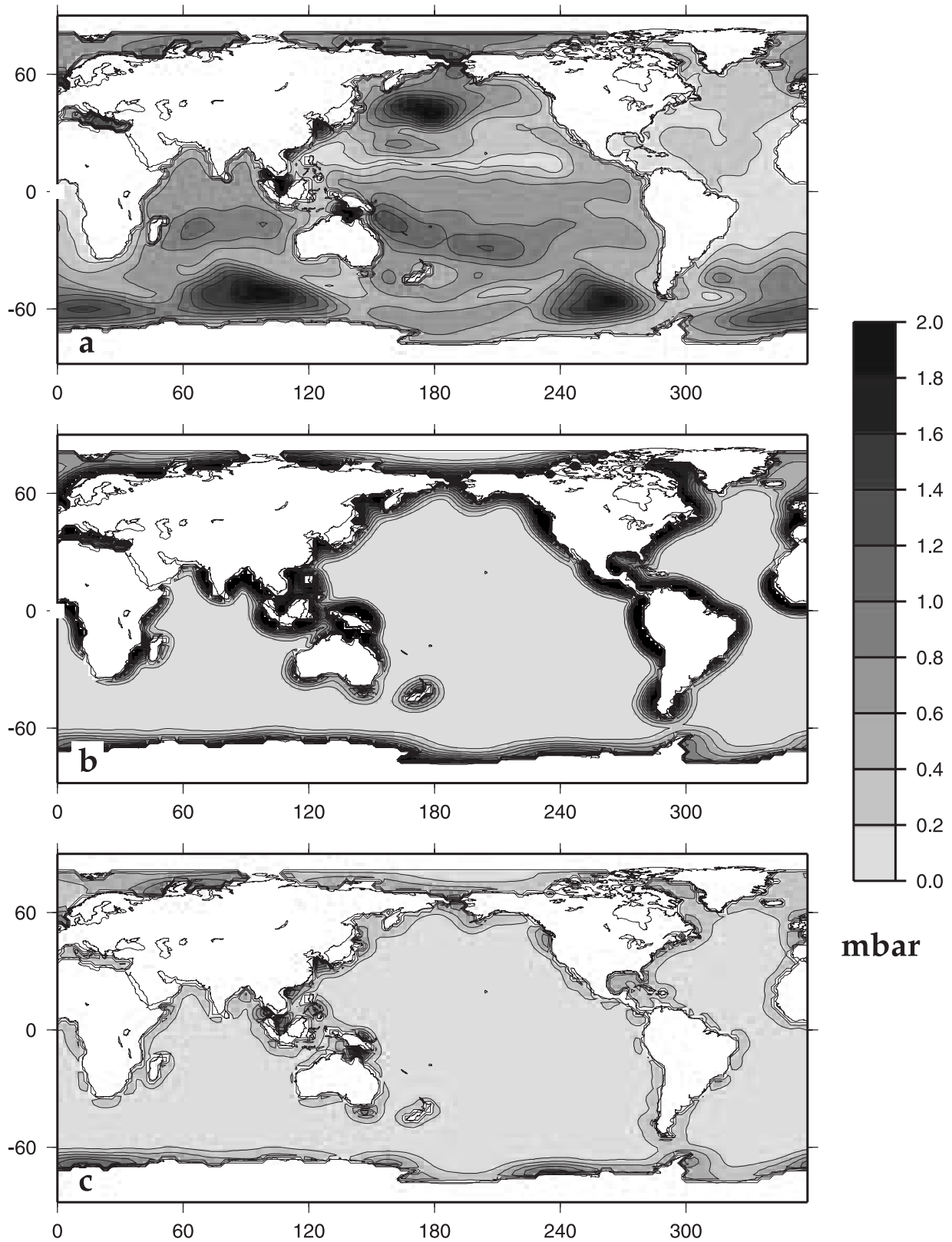
Figure 8. A map of the RMS, about the mean, of 30-day averages, spatially smoothed with a 500 Gaussian averaging function, of: (a) the POP bottom pressure fields; (b) the GRACE recovery error for bottom pressure; (c) the GRACE recovery error for bottom pressure, after applying the algorithm described in the text to reduce the contamination caused by mass variability on continents.
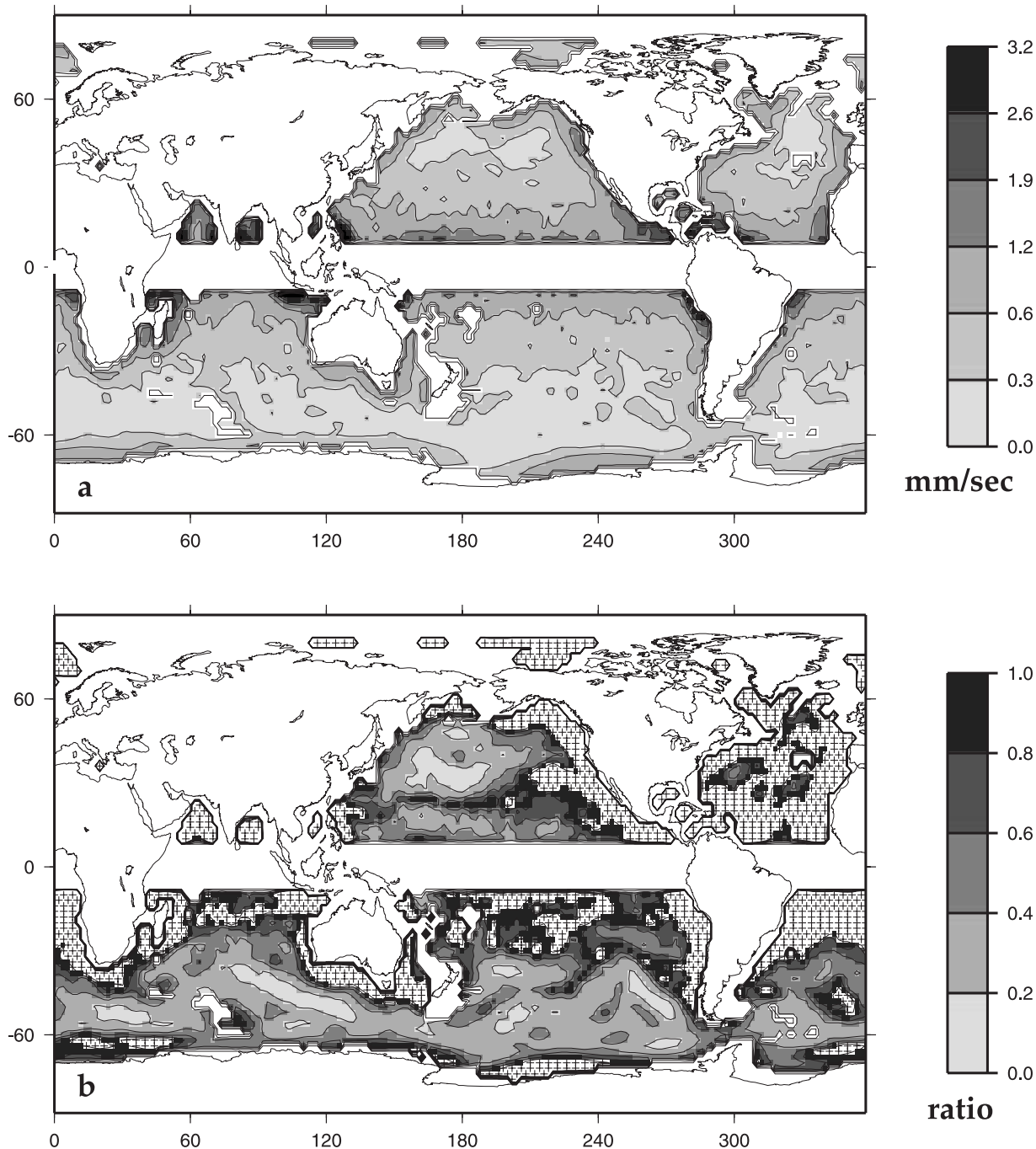
Figure 9. (a) A map of the RMS, about the mean, of the amplitude of the GRACE recovery errors for 2125 m currents. The algorithm described in the text has been used to reduce the contamination from mass variability over land. (b) the ratio of the RMS values of the GRACE recovery errors (shown in panel (a)), to the RMS values of the correct amplitudes (shown in Figure 7a). The regions with the plus signs have recovery errors that are larger than the signal.

section 3. We first remove, however, all secular contributions over the one year time span, to avoid the complications caused by leakage of the unknown PGR signal into the GRACE estimates.

[46] We compute the vector difference between the currents recovered from the simulated GRACE data and the correct POP currents at 2125 m depth, and find the amplitude of that difference at every grid point. Figure 9a shows the RMS values of those amplitudes, after the continental mass signal has been reduced using the method described in section 3.3. The GRACE estimates along the coast are still limited by contamination from the hydrology signal. And at low latitudes, where the cos θ in the denominators of (18) and (19) is small, the GRACE measurement errors cause significant degradation of the velocity estimates.
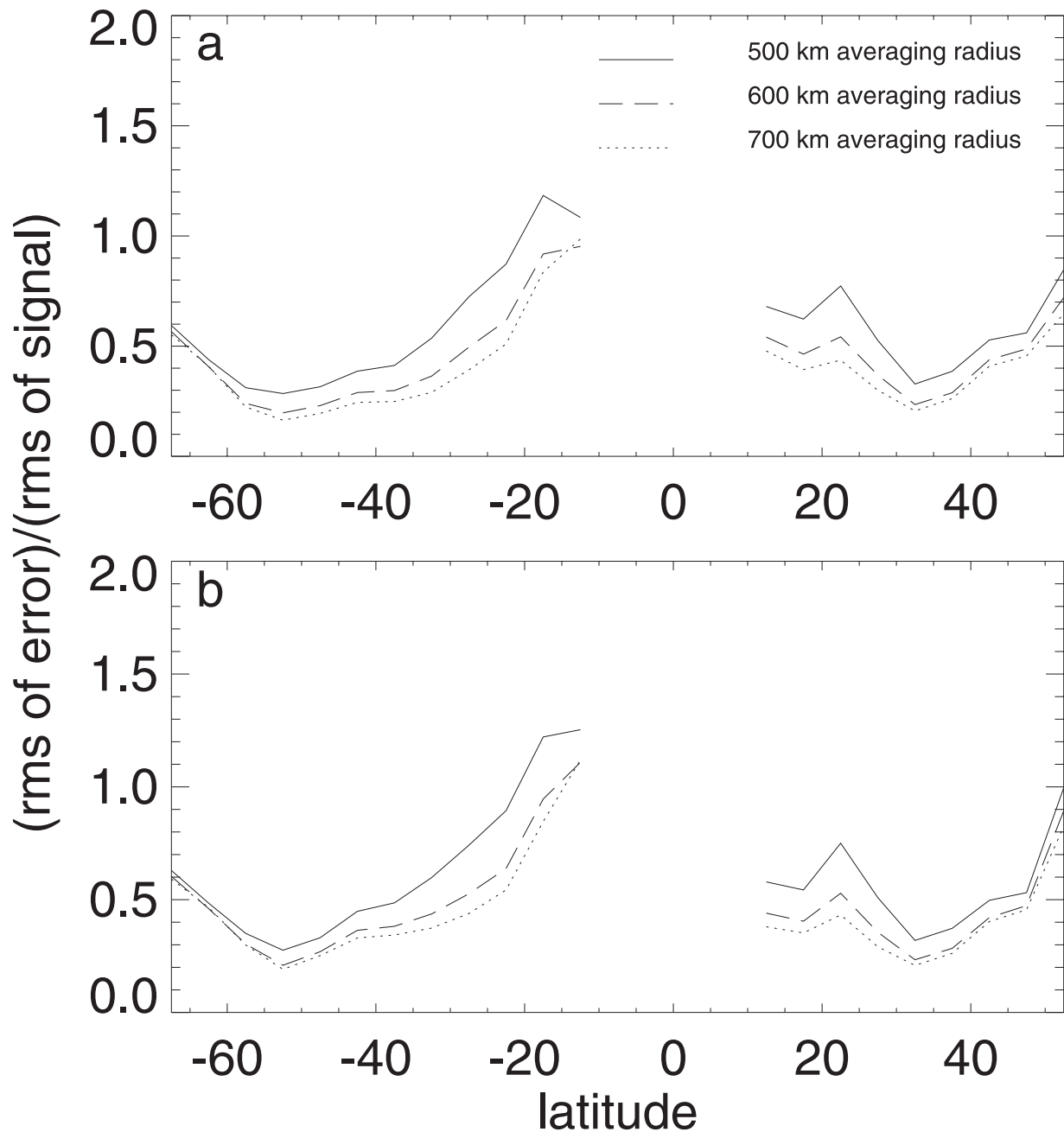
Figure 10. The ratio of the RMS of the GRACE recovery errors to the RMS of the variations in the currents themselves, for two depths: (a) 2125 m; and (b) 3125 m. Results are shown as a function of latitude and for three averaging radii.

[47] A comparison of Figure 9a with the RMS of the correct amplitudes shown in Figure 7a, suggests that the GRACE recovery error is significantly smaller than the signal throughout the Southern Ocean and much of the northern Pacific. This is illustrated more clearly in Figure 9b, which shows the ratio of the GRACE recovery error RMS (Figure 9a) to the RMS of the correct amplitudes (Figure 7a). The regions with the plus signs have recovery errors that are larger than the signal.

[48] Figure 10 shows the ratio of the RMS of the GRACE recovery error to the RMS of the currents, as a function of latitude and for 3 different Gaussian averaging radii. Only points that are further than 500 km from a continental coast are included when computing the RMS values. Figure 10a shows this RMS ratio for currents at a depth of 2125 m, and Figure 10b at a depth of 3125 m. Thus, the solid line in Figure 10a is a latitude average of the results shown in Figure 9b, except that Figure 9b also includes points within 500 km of the coast.

[49] Note, by comparing Figure 10a and Figure 10b, that the results at the two depths are similar, implying that GRACE should be able to deliver changes in currents at 2 km depth about as well as at 3 km depth. This is in contrast to the results of Figure 5b, that show the bottom geostrophic approximation does a significantly better job of reproducing the currents at 3 km depth than at 2 km depth.

The implication is that the accuracy of the GRACE recovery of currents at these depths is limited by the GRACE measurement errors.

[50] Increasing the Gaussian averaging radius decreases the effects of these measurement errors, and so improves the GRACE recovery. This is evident from the decreasing RMS ratio in Figure 10 as the averaging radius is increased. Note, from Figure 10, the good results at midlatitudes compared with the poorer results at low and high latitudes. When the estimates at 2125 m depth are integrated over latitudes between 30° and 50° (combining the northern and southern hemispheres), the ratio of the RMS of the recovery error to the RMS of the signal is about 0.4, 0.3, and 0.25 for 500 km, 600 km, and 700 km averaging radii, respectively. (When integrated over all latitudes greater than 10°, the ratios are about 0.6, 0.5, and 0.4 for radii of 500 km, 600 km, and 700 km, respectively.)

5. Summary

[51] In this paper we develop a method of inferring monthly changes in deep ocean currents using GRACE measurements of the Earth's time-variable gravity field. Briefly, GRACE provides estimates of changes in bottom pressure every 30 days. It is tempting to use those estimates to try to directly infer changes in currents at the seafloor, by assuming geostrophy. However, owing to the spatial smoothing that must be applied to the GRACE data confounded by the bottom topography, true bottom current estimates would be difficult to interpret. Instead, because we find good agreement between pressure variations at the seafloor and those up to depths as shallow as $\approx$2 km, we propose that the GRACE gravity measurements could be better used to infer monthly changes in currents at those depths.

[52] The spatial resolution of the current estimates are limited by the GRACE measurement errors, which increase with decreasing wavelength. We describe a smoothing process that reduces the effects of those errors by averaging the currents using a Gaussian function with an adjustable radius. Using simulated GRACE gravity data based in part on the POP model output (but ignoring possible contamination of the GRACE 30-day averages caused by temporal aliasing), we are able to obtain accurate results by choosing the averaging radius to be 500 km or larger. Because changes in the currents have most of their power at shorter scales than this, this smoothing process removes most of the signal. For example, for a 500 km radius the global RMS of the smoothed currents at 2 km depth is only about 30% of that of the unsmoothed currents, corresponding to about 10% of the variance. For 700 km, the RMS and variance ratios have decreased even further, to 24% and 6%, respectively.

[53] But an averaging radius this large does reduce the impact of the GRACE measurement errors to the point where the smoothed currents can be accurately recovered using the GRACE data. The recovery is best at midlatitudes and a few hundred km or more from the coasts. Near coastlines, the estimates suffer from contamination from the hydrological mass signal over land. Near the equator, where the Coriolis force is small, the remaining GRACE measurement errors lead to relatively large errors in the geostrophic estimates.

[54] But between latitudes of 30° and 50°, and more than 500 km from coastlines, our simulations suggest that the RMS of the GRACE recovery errors for changes in the currents at 2 km depth are about 40% of the RMS of the smoothed signal for a 500 km averaging radius, and about 25% for a 700 km radius. These results correspond to the recovery of the variance of the smoothed signal to about 15% and 6%, respectively. This relative error is especially small in the Southern Ocean and over much of the northern Pacific.

[55] The GRACE recovery errors in this midlatitude region are still dominated by the GRACE measurement errors, rather than by the hydrological contamination, or by the size of the nongeostrophic signal, or by the difference between the bottom pressure variations and those at 2 km depth. Because the GRACE measurement errors have the same effect on the recovery of currents at any depth, the current estimates at levels deeper than 2 km are not significantly better than the estimates at 2 km.

[56] One possible application of these data will be to combine them with in situ velocity observations from the profiling floats used in the Argo float program [*Roemmich and Owens*, 2000]. The float data will provide estimates of the time-mean and time-varying currents, but will suffer from sparse coverage and eddy aliasing problems. The satellite observations should allow for a more complete spatial coverage to fill in gaps in the float data, but will only provide the time-varying component of the large-scale circulation. Together, they offer the potential of providing a more complete picture of ocean circulation.

[57] Our conclusions about the ability of GRACE to recover bottom pressure and deep ocean currents, are based on the assumption that the errors in the GRACE 30-day Stokes' coefficients are determined entirely by instrumental accuracy. But there will almost certainly be additional errors, caused by short period geophysical signals being aliased into the 30-day averages. Potentially the most serious aliasing will be from short-period barotropic motion in the ocean [*Stammer et al.*, 2000; *Tierney et al.*, 2000; *Gille and Hughes*, 2001].

[58] Preliminary estimates (S. Bettadpur, personal communication, 1999) suggest that if nothing is done to reduce the effects of aliasing, the impact on the 30-day GRACE ocean estimates could be severe. The recovery errors for 500-km Gaussian averages of bottom pressure, for example, could well be on the order of 1 to 1.5 mbar—about an order of magnitude larger than the estimated errors shown in Figure 8c.

[59] The GRACE project will attempt to reduce these errors by using output from a barotropic ocean model to remove these aliasing signals from the GRACE measurements, before constructing the 30-day values. Furthermore, methods are being developed to further reduce the remaining aliased signal during the gravity field solution process. These efforts will continue as GRACE data are acquired. It may be well after launch before the full capabilities of GRACE can be realized.

References

Briegleb, B. P., and D. H. Bromwich, Polar climate simulation of the NCAR CCM3, *J. Clim.*, *11*, 1270–1281, 1998.

Chao, B. F., and R. S. Gross, Changes in the Earth's rotation and low-degree gravitational field induced by earthquakes, *Geophys. J. R. Astron. Soc.*, *91*, 569–596, 1987.

Chave, A. D., D. S. Luther, and J. H. Filloux, The barotropic electromagnetic and pressure experiment, 1, Barotropic current response to atmospheric forcing, *J. Geophys. Res.*, *97*, 9565–9593, 1992.

Dickey, J. O., et al., *Satellite Gravity and the Geosphere: Contributions to the Study of the Solid Earth and Its Fluid Envelope*, 112 pp., Natl. Acad. Press, Washington, D. C., 1997.

Dukowicz, J. K., and R. D. Smith, Implicit free-surface method for the Bryan–Cox–Semtner ocean model, *J. Geophys. Res.*, *99*, 7991–8014, 1994.

Gent, P. R., and J. C. McWilliams, Isopycnal mixing in ocean circulation models, *J. Phys. Oceanogr.*, *20*, 150–155, 1990.

Gille, S. T., and C. W. Hughes, Aliasing of high-frequency variability by altimetry: Evaluation from bottom pressure recorders, *Geophys. Res. Lett.*, *28*, 1755–1758, 2001.

Jekeli, C., Alternative methods to smooth the Earth's gravity field, *Rep. 327*, Ohio State Univ. Press, Columbus, 1981.

Jet Propulsion Laboratory, GRACE Science and Mission Requirements Document, GRACE 327-200, Rev. D, *JPL Publ.*, *D-15928*, 2001.

Johnson, T. J., C. R. Wilson, and B. F. Chao, Non-tidal oceanic contributions to gravity field changes: Predictions of the POCM, *J. Geophys. Res.*, *106*, 11,315–11,334, 2001.

Large, W. G., J. C. McWilliams, and S. C. Doney, Oceanic vertical mixing: A review and a model with nonlocal boundary layer parameterization, *Rev. Geophys.*, *32*, 363–403, 1994.

Large, W. G., G. Danabasoglu, S. C. Doney, and J. C. McWilliams, Sensitivity to surface forcing and boundary layer mixing in a global ocean model: Annual mean climatology, *J. Phys. Oceanogr.*, *27*, 2418–2447, 1997.

Ponte, R. M., A preliminary model study of the large-scale seasonal cycles in bottom pressure over the global ocean, *J. Geophys. Res.*, *104*, 1289–1300, 1999.

Roemmich, D., and W. B. Owens, The Argo Project: Global ocean observations for understanding and prediction of climate variability, *Oceanography*, *13*, 45–50, 2000.

Smagorinsky, J., General circulation experiments with the primitive equations, I, The basic experiment, *Mon. Weather Rev.*, *91*, 99–164, 1963.

Smith, R. D., and J. C. McWilliams, Anisotropic viscosity for ocean models, *Ocean Modell.*, Hooke Inst. Oxford Univ., Oxford, England, in press, 2002.

Stammer, D., C. Wunsch, and R. Ponte, De-aliasing of global high frequency barotropic motions in altimeter observations, *Geophys. Res. Lett.*, *27*, 1175–1178, 2000.

Swenson, S., and J. Wahr, Estimated effects of the vertical structure of atmospheric mass on the time-variable geoid, *J. Geophys. Res.*, *107*(B9), 2194, doi:10.1029/2000JB000024, 2002.

Tierney, C., J. Wahr, F. Bryan, and V. Zlotnicki, Short-period oceanic circulation: Implications for satellite altimetry, *Geophys. Res. Lett.*, *27*, 1255–1258, 2000.

Wahr, J., M. Molenaar, and F. Bryan, Time-variability of the Earth's gravity field: Hydrological and oceanic effects and their possible detection using GRACE, *J. Geophys. Res.*, *103*, 30,205–30,230, 1998.

Wunsch, J., M. Thomas, and T. Gruber, Simulation of oceanic bottom pressure for gravity space missions, *Geophys. J. Int.*, *147*, 428–434, 2001.

———————————

F. O. Bryan, National Center for Atmospheric Research, Climate and Global Dynamics Division, PO Box 3000, Boulder, CO 80307-3000, USA. (bryan@cgd.ucar.edu)

S. R. Jayne, Physical Oceanography Department, Woods Hole Oceanographic Institution, MS 21, Woods Hole, MA 02543-1541, USA. (sjayne@whoi.edu)

J. M. Wahr, Department of Physics and Cooperative Institute for Research in Environmental Sciences, University of Colorado, Campus Box 390, Boulder, CO 80309-0390, USA. (wahr@lemond.Colorado.edu)